Extended Abstracts of the 2006 International Conference on Solid State Devices and Materials, Yokohama, 2006, pp. 438-439

P-1-19

Nitrogen Induced Extrinsic States (NIES) in Effective Work Function Instability of TiN_x/SiO_2 and TiN_x/HfO_2 Gate Stacks

Chao-Sung Lai[1], Jer-Chyi Wang[2], Shih-Cheng Yang[1], Jian-Yi Wong[1], Shing-Kan Peng[1]

[1]Department of Electronic Engineering, Chang Gung University,
259 Wen-Hwa 1st Road, Kwei-Shan Tao-Yuan 333, Taiwan
[2]Nanya Technology Corporation, Hwa-Ya Technology Park,
669 Fu-Hsing 3rd Rd, Kueishan, Taoyuan, Taiwan
Phone: +886-3-2118800 ext. 5786 E-mail: cslai@mail.cgu.edu.tw

1. Introduction

As the scaling of channel length and gate oxide thickness, the metal gate electrodes will be required [1-2] due to severe poly depletion effects, high gate resistance, and boron penetration for poly-Si gate electrode. In addition, Fermi-level pinning at metal/dielectrics interface is easily observed [3], which will induce threshold voltages instability. In this work, we investigated the nitrogen induced extrinsic states (NIES) leading to the effective work function (Φ_m) instability of TiN_x/SiO_2 and TiN_x/HfO_2 gate stacks. The Fermi-level pinning effect of TiN_x/HfO_2 gate stacks was nearly negligible. However, for the TiN_x/SiO_2 gate stack, the Φ_m was pinned at about 4.8 and 4.3eV for TiN_x with low (0%~6%) [3] and high N_2% (10%~12%) respectively. The extra nitrogen in TiN_x induced some extrinsic states at TiN_x/SiO_2 interface is responsible for the Φ_m instability.

2. Experiments

Typical HfO_2 and SiO_2 capacitors with TiN_x metal gate were fabricated in this study. The SiO_2 with film thickness ranged from 10 to 50nm were grown by thermal oxidation on p-type silicon wafer, and the HfO_2 films were deposited by r.f. magnetron sputtering system. After the dielectrics had been formed, TiN_x (100nm) gate electrode was deposited by DC-sputter at 250W in N_2 and Ar mixtures, with N_2 flow ratio from 0% to 12%, respectively. TiN_x gate was then patterned by wet etch using the chemicals of $NH_4OH:H_2O_2$=1:2. Some samples were rapid thermal annealed at 500 to 700°C in N_2 ambient for 30sec.. Finally, 300nm Al films were deposited on backside contact and sintering in N_2 ambient at 400°C for 30min. The detailed process flow and capacitor cross-section were shown in Fig. 1(a) and (b) respectively. For thermal stability study, the TiN_x thin films deposited on 50nm oxides were prepared also. Besides, the capacitance-voltage (C-V) curves and resistivity of TiN_x films were measured by HP4285 LCR meter and four point-probe meter, respectively.

3. Results and Discussion

A. Material and electrical characterization

Fig. 2 shows the resistivity of TiN_x films with different sputtered N_2 flow ratio and PMA temperature. The resistivity of TiN_x increased from 2×10^{-4} to 6.93×10^{-4} Ω-cm for all nitrogen ratios and nearly not affected by PMA. The XRD analysis is shown in Fig. 3. In this figure, we can observe that Ti(011) in pure Ti film diminished when nitrogen incorporated, and TiN(111) became dominant in TiN_x films with increasing N_2 flow ratio [4].

The C-V curves of TiN_x/SiO_2 gate stacks with different sputtered N_2 flow ratio are shown in Fig. 4. In order to decouple the effect of oxide charge from the effective work function, the capacitors with different oxide thicknesses were fabricated to generate a V_{FB} vs. EOT curve as shown in the inset of Fig. 5. The y-intercept of this curve indicated the effective work function (Φ_m). The extracted Φ_m values for TiN_x gate electrode with different N_2 flow ratio ranged from 4.0 (low N_2) to 4.9eV (high N_2) are shown in Fig. 5. This suggests that TiN_x films have tunable effective work functions appropriate for both NMOS and PMOS devices.

B. Nitrogen induced extrinsic states (NIES)

Fig. 6 shows the PMA temperature dependence of V_{FB} for TiN_x/SiO_2 gate stacks with different sputtered N_2 flow ratio. We can observe that the Fermi-level pinning effect is quite different for low and high nitrogen ratio. The effective work function (Φ_m) extracted by different oxide thickness is shown in Fig. 7. The Φ_m for low N_2 flow ratio of TiN_x (2%~6%) was pinned at about 4.8eV [3], while pinned at about 4.3eV for the high one (10%-12%). Nevertheless, we did not observe any pinning effect at TiN_x/HfO_2 gate stacks as shown in Fig. 8. We can rationally suggested that some nitrogen induced extrinsic states (NIES) near the silicon conduction band were formed when nitrogen ratio up to 10% [5]. To further investigate this, the effective barrier height ($q\Phi_B$) of SiO_2 gate dielectrics with TiN_x metal gate of different N_2 flow ratio was extracted based on F-P emission as shown in Fig. 9 and summarized in Table 1. The NIES was formed for the high nitrogen ratio. Fig. 10 shows the models of a metal-dielectric interface structure for low and high N_2 flow ratio of TiN_x. According to pinning effect of TiN_x (10%), we can conclude that there was some NIES formation near the silicon conduction band.

4. Conclusion

In this paper, the effective work function instability of TiN_x/SiO_2 and TiN_x/HfO_2 gate stacks has been developed. For low N_2 flow ratio of TiN_x/SiO_2 gate stacks, the Φ_m was pinned at about 4.8eV, while pinned at 4.3eV for the high one. However, the pinning effect was almost negligible for TiN_x/HfO_2 gate stacks. The nitrogen induced extrinsic states (NIES) will contribute to the Φ_m instability and the energy band diagrams were also proposed to explain it.

Acknowledgement

This work was support by the National Science Council under the contract of NSC 94-2215-E-182-008.

Reference

[1]IRTS, Semiconductor Industry association, San Jose, CA, 2005.
[2]Cho Sung Lai et al., ALD Conference, Finland, 2004.
[3]H. Y. Yu et al., IEEE Electron Device Letters, vol. 25, 2004
[4]M. Kawamura et al, Thin Solid Films 287 (1996) 115-119
[5]X. R. Cheng et al, J. Appl. Phys, 63, 797, (1998).

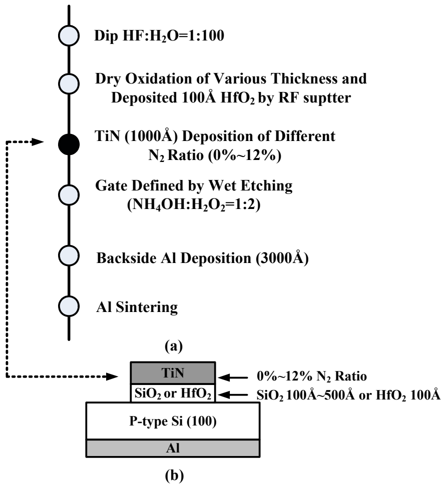

Fig.1 (a) The process flow of TiN_x metal gate MOS capacitors. (b) Schematic cross-section for TiNx metal gate MOS capacitors in this work.

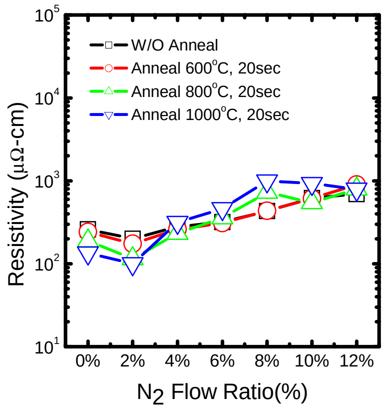

Fig. 2 Influence of the N_2 flow ratio on the resistivity of the TiN_x films deposited on the silicon oxide.

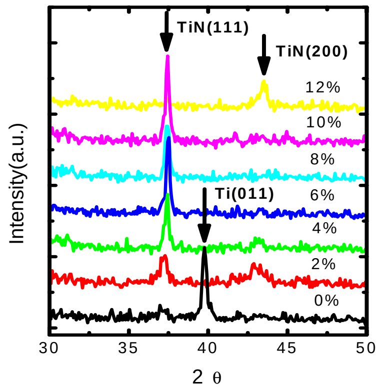

Fig. 3 XRD patterns of the TiN_x films with various N_2 flow ratio.

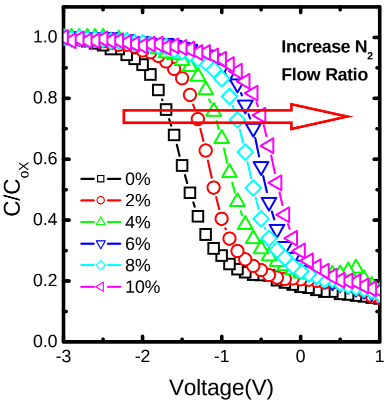

Fig. 4 Normalize C-V curves of TiN_x gates with various N_2 flow ratio on SiO_2/p-type Si.

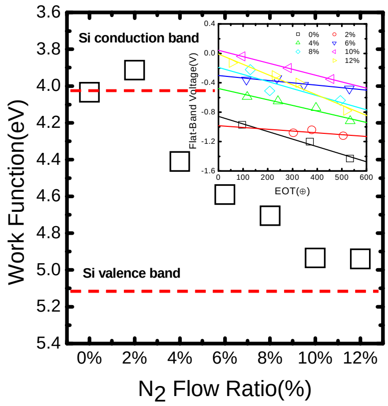

Fig. 5 Work function of TiN_x as a function of the N_2 flow ratio (Φm= 4.0~4.9eV).

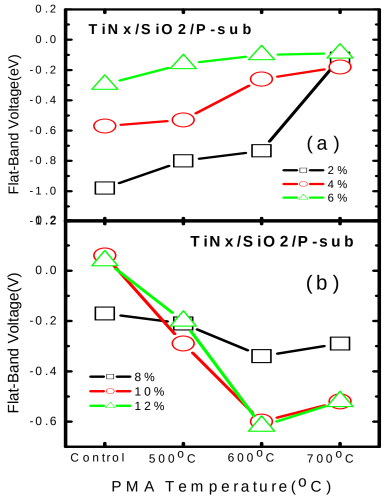

Fig. 6 V_{FB} vs. PMA temperature of TiN_x/SiO_2 gate stacks with different N_2 flow ratio.

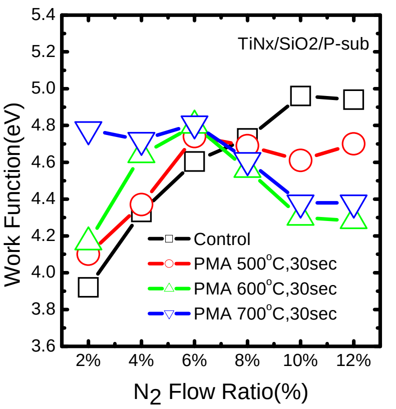

Fig. 7 Work function with different N_2 flow ratio of TiN_x/SiO_2 gate stacks under various PMA temperature.

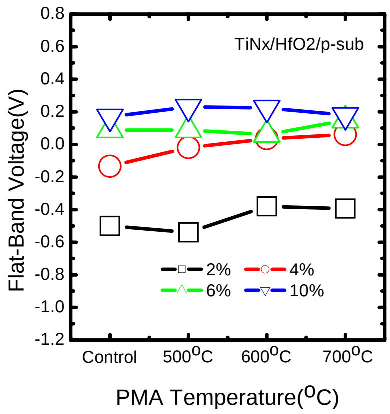

Fig. 8 V_{FB} vs. PMA temperature of TiN_x/HfO_2 gate stacks with different N_2 flow ratio.

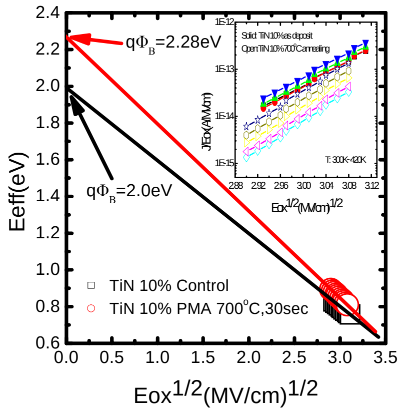

Fig. 9 The F-P barrier height from the dependence of effective activation energy, $E_{eff}=q[\Phi_b-(qE_{ox}/\pi\varepsilon_i)^{1/2}]$, on the square root of electric field.

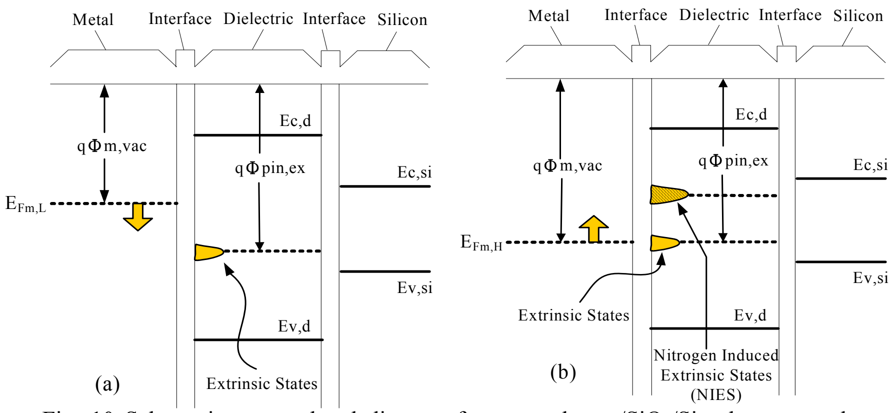

Fig. 10 Schematic energy band diagram for a metal gate/SiO_2/Si substrate stacks, showing extrinsic states that pin the metal Fermi-level. (a) Extrinsic state near Ev,si for TiN_x (2%-6%) . (b) Nitrogen Induced Extrinsic states (NIES) near Ec,si for TiN_x (10%-12%).

Table 1. Summary of the effective barrier height of these samples with different N_2 flow ratio b/a PMA.

TiN_x Split	**$q\Phi_B$ (eV)**	**$\Delta q\Phi_B$ (eV)**
4% as-dep.	2.22	0.08
4% 700°C PMA	2.30	
10% as-dep.	2.0	0.28
10% 700°C PMA	2.28	